BBC RD 1980/11

RESEARCH DEPARTMENT REPORT

Colour operation of a solid state sensor telecine

Dr. I. Childs

Research Department, Engineering Division
THE BRITISH BROADCASTING CORPORATION
November 1980

BBC RD 1980/11
UDC 621.377.6
621.385.832.5
771.531

COLOUR OPERATION OF A SOLID STATE SENSOR TELECINE

Dr. I. Childs

Summary

An experimental colour film scanner has been constructed using solid state CCD image sensors. Such a scanner should give improved reliability and ease of maintenance together with good picture quality. Various technical aspects of performance are discussed and the picture quality is shown to be in most respects at least as good as that of a flying spot scanner. One possible exception is the noise level, which is marginal; however, foreseeable improvements in solid-state sensor design, should overcome this problem.

Issued under the authority of

Head of Research Department

Research Department, Engineering Division,
BRITISH BROADCASTING CORPORATION
(November 1980)
(PH-217)

COLOUR OPERATION OF A SOLID STATE SENSOR TELECINE

(PH-217)

COLOUR OPERATION OF A SOLID STATE SENSOR TELECINE

Dr. I. Childs

1. Introduction

For some years, work has been in progress to study the feasibility of using single-line solid state image sensor arrays for scanning film. This work started in 1973 with the use of a 512-element photodiode array;[1,2] since then different types of array have been investigated culminating in the use of CCD sensors.[3,4] The first section of this report will describe results obtained from a monochrome film scanner using one of these devices with 1024 sensing elements. The additional requirements of a colour film scanner will then be discussed together with results obtained using three of these CCDs.

The optical system used in all the monochrome tests is shown in Fig. 1. A capstan moves the film at constant speed past a light source (a quartz halogen lamp was used for all the experiments). An image of the film is formed on the sensor by a copying lens, the sensor forming a television signal line by line. Such an arrangement necessarily produces sequentially scanned images; these are incompatible with an interlaced transmission system (see Fig. 2). In order to display the signals conventionally, therefore, they must first be converted to interlaced form. While this sequential-to-interlace conversion could be avoided by mechanical means (e.g. moving mirrors or rotating polygons), a digital processor using a field store avoids mechanical and optical complication, provides easier maintenance, freedom from flicker, and eliminates the possibility of positional errors between odd and even fields.

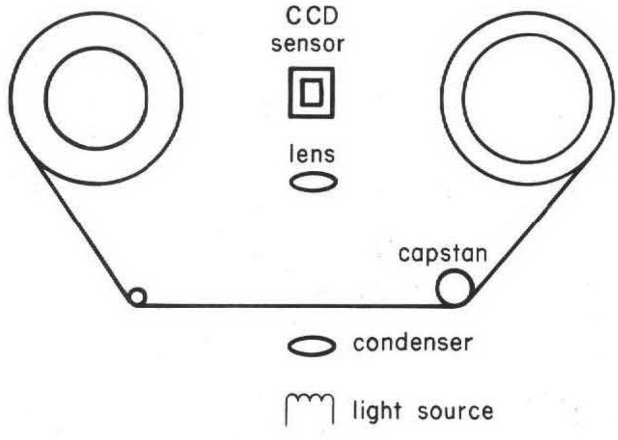

Fig. 1 - Simplified layout of monochrome CCD telecine

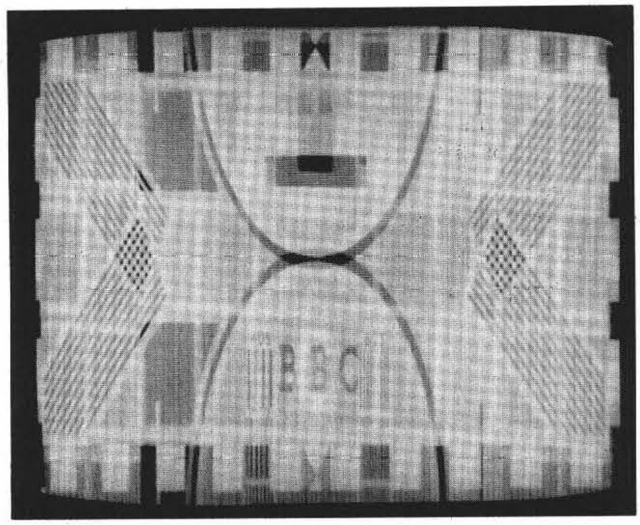

Fig. 2 - Output of CCD before sequential-to-interlace conversion

2. Operation of charge-coupled devices

Although the detailed physics of the construction and operation of charge-coupled devices is outside the scope of this report, a brief description will be given in order to enable the reader who is unfamiliar with this subject to understand some of the later sections. For further information the reader is referred to some of the excellent books on the subject.[5]

Fig. 3(*a*) shows the construction of a three-phase charge-coupled device. It consists of a p- or n-type channel in the silicon substrate; covering this channel, but insulated from it by a thin layer of silicon oxide, are three sets of electrodes. If the appropriate voltage is applied to one set of electrodes a series of potential wells is formed in the channel beneath them and minority carriers injected into these wells are unable to leave and are thus stored.

If the positions of the wells are altered by varying the voltages on the three sets of electrodes as in Figs. 3(*b*) and 3(*c*), the stored charges can be moved along the channel. The CCD thus behaves as an analogue shift register, so that charges initially in each of the wells may be moved along the register to one end, at which point they may be fed to an output circuit.

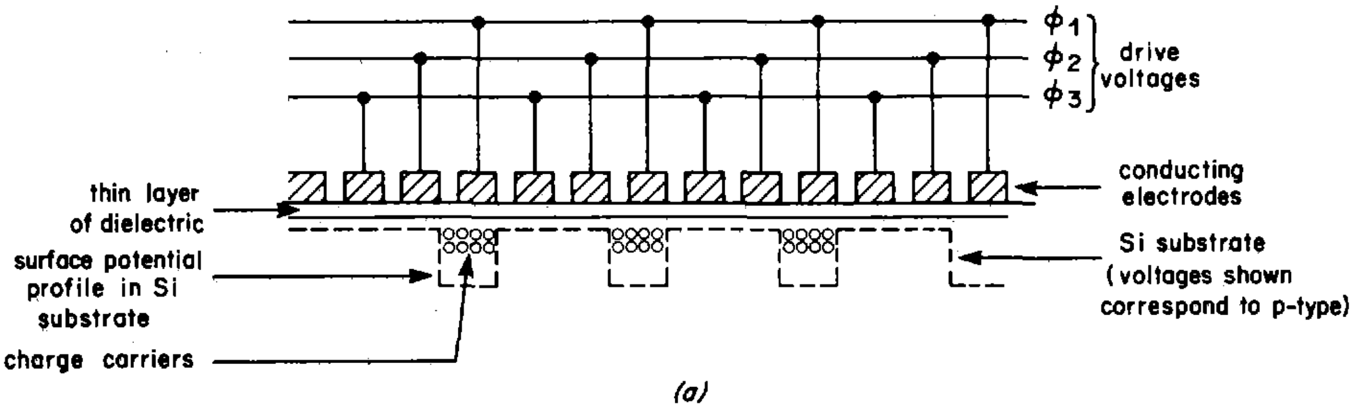

Fig. 3 - Construction and operation of 3-phase CCD

(a) ϕ_1 voltage positive, ϕ_2 and ϕ_3 voltages zero (b) ϕ_2 taken positive, ϕ_1 and ϕ_3 unchanged (c) ϕ_2 remains positive, ϕ_1 taken to zero

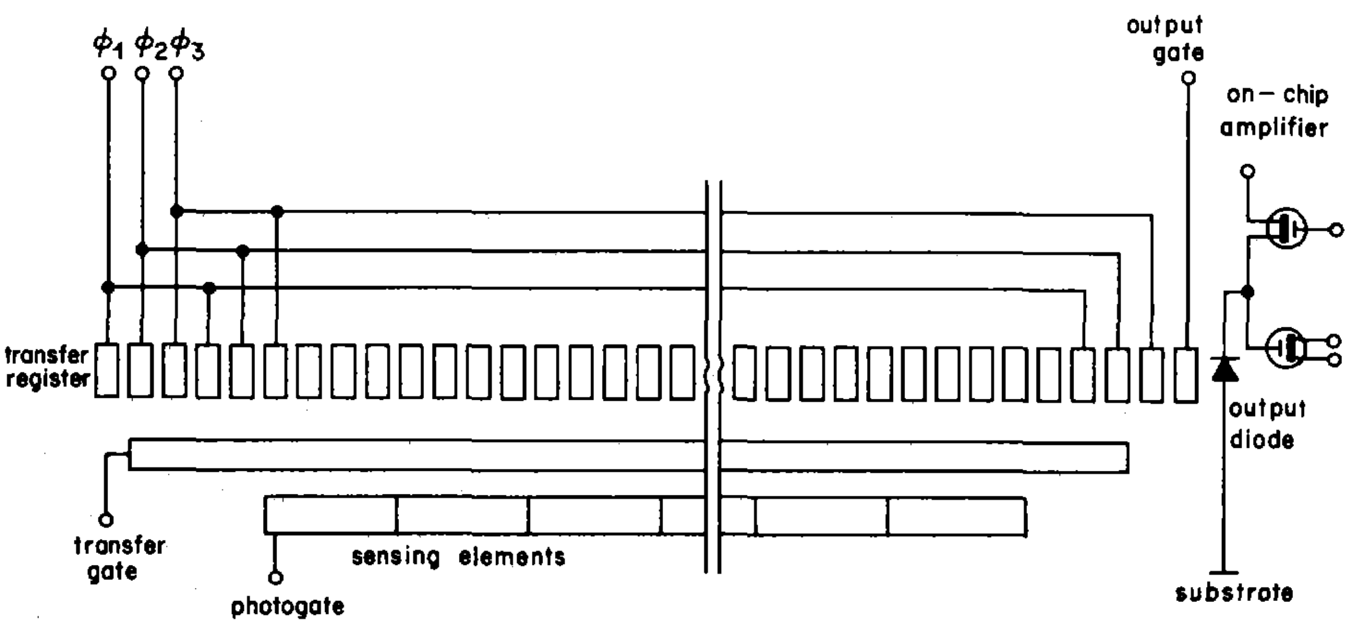

Fig. 4 - Layout of a typical linear sensor array

The charges may enter the wells either from an input gate or by carriers released when light is allowed to fall on the substrate. It is this latter effect which is used in image-forming applications. Fig. 4 shows an arrangement commonly used in single-line arrays. Light falling on the image sensing elements releases charge which is stored in potential wells underneath each element. Once per television line the contents of all the individual elements are simultaneously passed to corresponding elements in a transfer register. While the next charge image is being formed under the image sensing elements, the contents of the transfer register are read out in sequence, and form an electrical signal. The two parts of the CCD thus perform the image sensing and one of the scanning functions required to produce a television waveform.

There are several variations possible. If the profile of the potential wells in the channel is made asymmetric, either by implanting impurities or by varying the thickness of the oxide layer, it is possible to achieve charge transport with only two clock phases instead of three.[6,7] This considerably simplifies the electrode structure by removing the need for one set to cross over another.

A second variation is the buried channel device.[8,9] In a surface-channel CCD, defects in the silicon trap some of the carriers so that not all the charge is transferred. The concentration of these defects is higher at the surface than in the bulk material. Thus, if the channel is formed below the surface of the substrate by additional diffusions during manufacture, the proportion of charge is transferred at each step is improved. An additional benefit obtained by increasing the spacing between the electrode structure and the channel is that the profile of the electric field from each electrode in the charge-carrying region is made more suitable for high-speed operation.

It should be noted at this point that the light must pass through the electrodes on the surface of the CCD. This is usually achieved by making them of some transparent material such as polysilicon. It will be shown later that this can cause problems and alternative techniques are now becoming available.

3. Performance of a monochrome film scanner

Initially one 1024 element buried channel CCD image sensor was purchased for evaluation; this sensor used 2 phase operation and was capable of producing a complete line scan within 64 μs.

The use of solid-state sensors in film scanners can potentially provide many advantages. Some of these are a reduction in size and complexity, complete absence of afterglow, no lag and long-term drift, an inherent absence of geometric distortion, no need for replacement on a regular basis, and the elimination of high voltages from the equipment. Nevertheless some problems remain and there are other problems that are unique to the use of CCDs; these problems will now be considered in detail.

3.1. Sampling

Each sensing element in a CCD averages the intensity of the incident light over a finite area to produce a single sample of the average illumination. The effect of the averaging is to cause some loss of response to high spatial frequencies; this will be considered more fully in the next section. The effect of the sampling is to produce alias components if the scene to be televised contains significant information at spatial frequencies above the Nyquist limit (corresponding to a spatial wavelength of two elements).

Fig. 5 shows the output of a 512-element photodiode array used in earlier tests. The Nyquist limit for this array was 5 MHz and it will be seen that there is no response at this frequency. The apparent response at 5.5 MHz is due to an alias component at 4.5 MHz. Among other things this indicates that 512-elements is not sufficient to reproduce pictures with a bandwidth of 5.5 MHz.

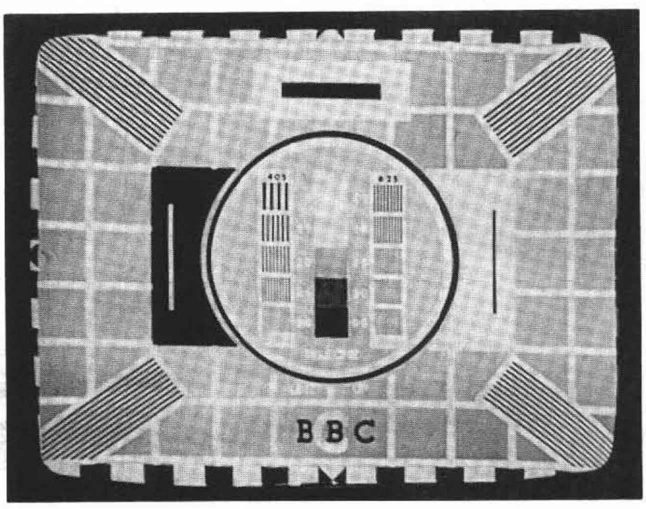

Fig. 5 - Output of a 512-element sensor

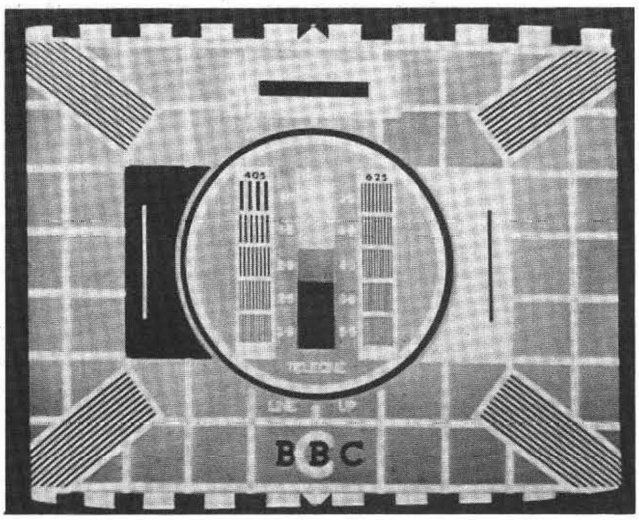

Fig. 6 - Output of a 1024 element CCD

In contrast, Fig. 6 shows the output of a 1024 element buried channel CCD sensor; no alias components are visible. This sensor was operated at a sampling rate of 17.8 MHz in order to give a line scan duration of 57 μs (i.e. approximately 10% overscan). At this rate the Nyquist limit is 8.9 MHz; however, any alias components produced by exceeding this limit are not visible until they fall below 5.5 MHz corresponding to a frequency before sampling of over 12.3 MHz. Bearing in mind the high frequency loss associated with the film camera lens, the film itself, the telecine copying lens and the sensor itself it is unlikely that there will be any significant information at these frequencies even with 35 mm film; in any case, even when using the 512-element sensor, aliasing was rarely visible on normal film material.[10]

It should be noted that, although a CCD is a sampled system, it behaves exactly as a conventional picture source if the output is passed through a low-pass filter. There is therefore no need to link the CCD sampling frequency with any other sampling frequency such as, for example, that which might be used in a digital signal processing channel.[10,11] Indeed, such a linking may be undesirable because the requirements of the two systems are not necessarily the same.

3.2. Spatial response

Light falling anywhere on a sensing element produces a signal in that element; ideally it produces no response elsewhere. Thus the response of that element as the position of the incident light is varied (the 'aperture' of the sensor) is as shown in Fig. 7(*a*). This implies a spatial frequency response of the sin x/x form as shown in Fig. 7(*b*), the response being 4 dB down at the Nyquist limit discussed above. The basic spatial frequency response may be further modified if there is lateral charge spreading in the sensing

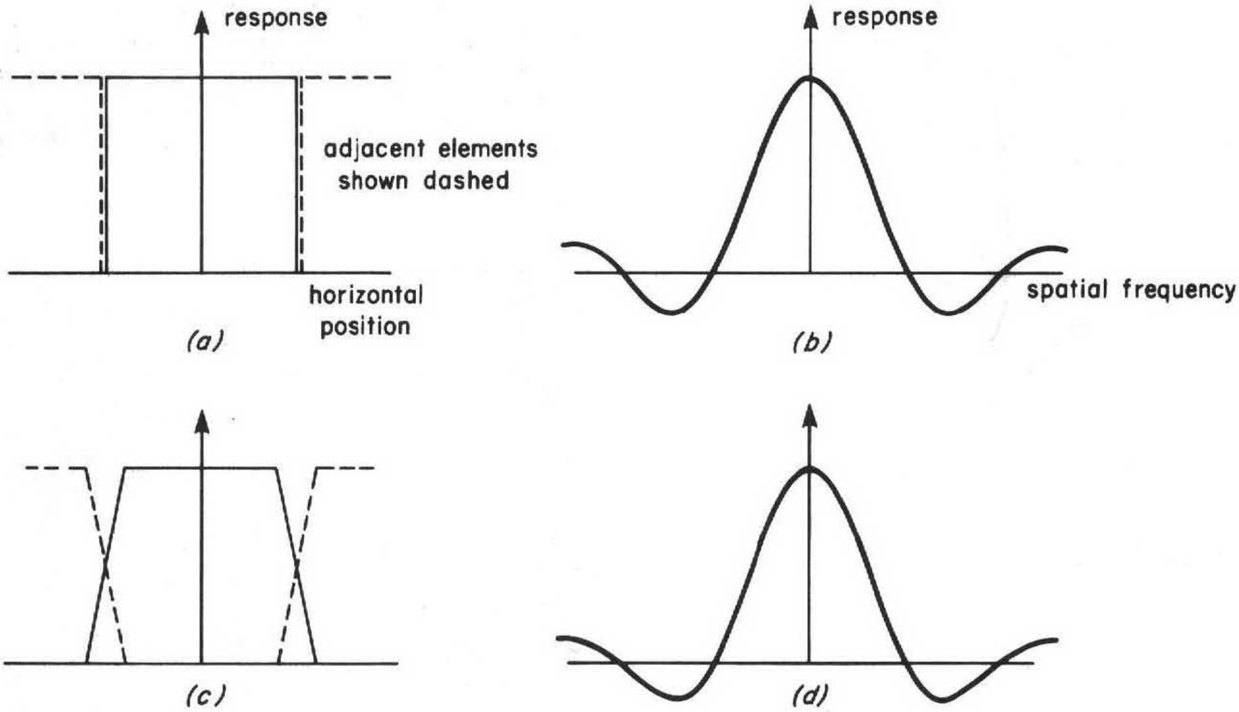

Fig. 7

(a) Aperture of ideal image sensor element
(b) Spatial frequency response of sensor with elements of aperture shown in (a)
(c) A more realistic element aperture
(d) Modified spatial frequency response corresponding to (c)

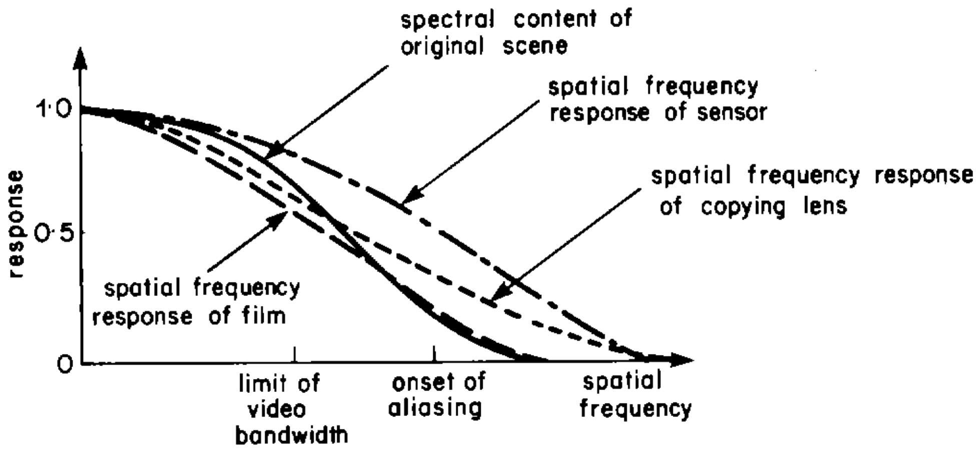

Fig. 8 - Factors contributing to horizontal spatial frequency response

register. Thus carriers released in the gap between elements may travel to either element; the effective aperture then becomes as shown in Fig. 7(*c*). For the degree of charge spreading that might be expected in practice (and measurements have indicated that this is very slight) the effect on the spatial frequency response is negligible. For example Fig. 7(*d*) shows the spatial frequency response caused by the sensor aperture of Fig. 7(*c*); comparison with Fig. 7(*b*) reveals only slight differences.

As a result of the effect illustrated in Fig. 7(*b*) the response of the sensor at horizontal spatial frequencies corresponding to 5.5 MHz is −1.4 dB with respect to that at zero frequency. This loss is small compared to those in the film and the copying lens. The response of 16 mm black and white film at 5.5 MHz was measured and found to be 56% (−5 dB) of its low frequency value; colour film will be even less. Likewise the copying lens introduces a further 3 dB of loss. These losses will all increase with spatial frequency, thus helping to attenuate any components likely to cause aliasing; the response of the sensor alone has dropped by a further 7 dB at 12.3 MHz. Fig. 8 illustrates how these losses might typically be associated with the basic response of the 1024 element sensor.

The vertical spatial response of the scanner is complicated by the motion of the film. The sensor integrates the film image for a whole line period; thus if the sensor elements were negligibly small the vertical aperture would have a width of one television picture line (referred to the final televised image). This is shown in Fig. 9(*a*). In practice, of course, each sensor element has a finite size; Figs. 9(*b*), 9(*c*) and 9(*d*) show the vertical apertures if the sensor elements are smaller than, equal to or wider than a television line

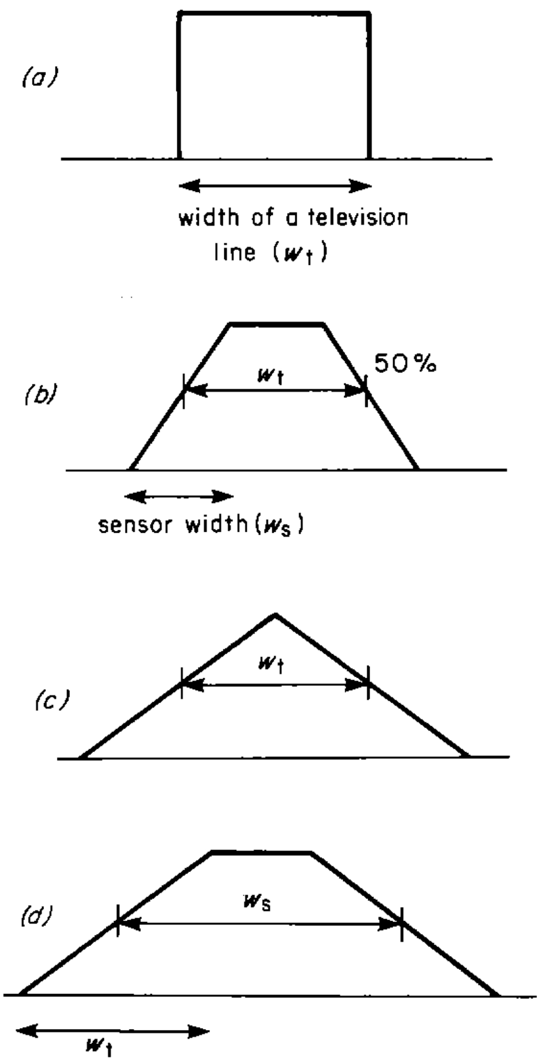

Fig. 9 - Vertical aperture of sensor/film scanner combination

(a) Negligibly small sensor elements
(b) Sensor elements smaller than a television line width
(c) Sensor elements the same size as a television line
(d) Sensor elements larger than a television line width

respectively (the width of a television line being in this instance, equal to the pitch or spacing between adjacent picture lines).

It can be shown that there is an optimum element size in the vertical direction (see Appendix I). Sensors with wider elements collect more light but require more aperture correction; this boosts the noise level and outweighs the gain in sensitivitity. The optimum element width is approximately 1.3 times the television line width, although there is an appreciable tolerance on this value. The 1024 element sensor has square sensing elements; thus if the image size is adjusted for 10% overscan the effective width of the sensor is 0.9 times the width of a television line; this gives a signal to noise ratio only 1.2 dB worse than optimum. The use of sensors to provide a film scanner with an optimum vertical aperture should result in very low grain visibility in the final picture.

3.3. Transfer loss

One of the defects of early CCD sensors was that not all the carriers moved with the potential wells. Some were trapped by defects in the silicon to be released at a later time. Thus after a large number of transfers some of the charge from a given element is 'smeared' into subsequent elements. The effect of this is to reduce resolution in a non-uniform way.[3] The left-hand side of the picture, having suffered fewer transfers, has more detail than the right-hand side.

It can be shown that the amplitude of a sine-wave emerging from a CCD is described by the expression

$$A_o = A_i \exp\left\{-n\epsilon\,(1-\cos 2\pi f/f_c)\right\} \qquad (1)$$

where A_i = amplitude of sine wave from an ideal sensor (i.e. one with no transfer loss)

A_o = amplitude of sine wave out of an actual sensor

n = number of electrode transfers

f = frequency of the sine wave

f_c = clock frequency of CCD

ϵ = proportion of charge left behind at each transfer

The transfer register of the 1024 element CCD used in the experiments is split into two halves. Each half receives the signal from alternate sensing elements; thus the CCD is organised as two interleaved 512-element sensors. This is done to minimise the clock frequencies and to ease fabrication. The clock frequency of each half is therefore half of the total sample rate (i.e. f_c = 8.9 MHz) and the charge from the extreme end of the sensor has only to pass through 512 stages. Each stage has two phases so n = 2 x 512 = 1024. The maximum frequency present in each half of the transfer register is 8.9/2 or 4.45 MHz. At this frequency:

$$\frac{A_o}{A_i} = \exp(-2048\epsilon) \qquad (2)$$

Even if ϵ is only 0.1%, A_o is attenuated by nearly 18 dB so it is clearly important to keep charge transfer loss to a minimum. This is one of the advantages of buried channel devices; they typically have charge transfer losses of one to two orders of magnitude lower than surface channel CCDs because of the lower defect density and improved speed capability.

In practice no change in resolution could be determined between the left- and right-hand sides of the picture even at 4.5 MHz. The experimental accuracy was estimated as better than 10%; if a 10% difference existed, concealed by the estimating error, the value of ϵ calculated from Equation (1) would be 5.1×10^{-5}.

3.4. Blooming

If the level of illumination in picture highlights is too high the charge contained in one well can spill over into adjacent wells. This is known as blooming, and the effect is shown in Fig. 10. Fortunately the maximum level of illumination available in a telecine machine is usually fixed (the open-gate level) and it can be arranged that this

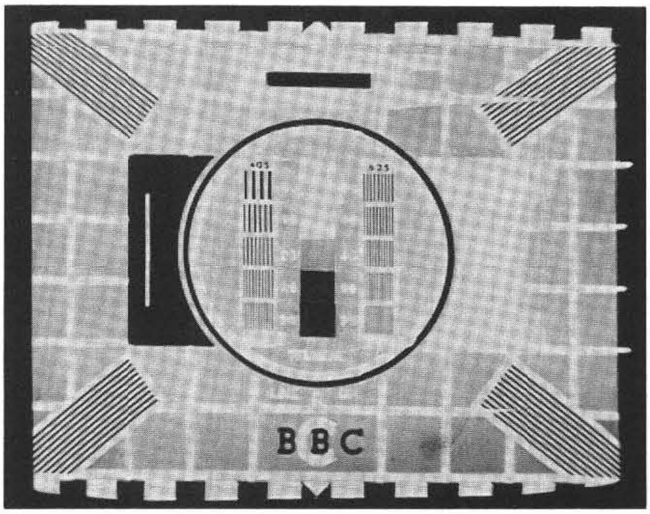

Fig. 10 - Effect produced by blooming

level is just less than that which would cause blooming. Under these conditions blooming would never occur. An exception would be, however, if the light level were increased in order to accommodate film of high minimum density. In this case blooming might possibly appear when reverting to more normal film.

There are techniques available in the design and manufacture of CCDs which can help control the blooming; this is another alternative but suitable sensors using these techniques are not yet available.

3.5. Dark current

At the opposite extreme, in the absence of light, there will still be a small signal from a CCD; this is due to the generation of carriers by random thermal activity in the silicon substrate and will cause an added 'dark current' signal in the output and an increase in noise. Not all the elements will have the same dark current and dark current 'spikes' may be seen (these are high values of dark current due to a fault in the substrate). All these effects are proportional to the time between scans; fortunately if the sensor is scanning at television line rate the dark current is small due to the comparatively short time between successive scans. The manufacturers specify a maximum average dark signal of 3% of peak voltage and a maximum deviation from this, for any single element, of 5% of peak voltage at an integration time of 768μs. At 64 μs integration these figures become 0.25% and 0.42% respectively.

This is a major advantage of CCDs over photodiode sensors. Photodiode sensors, in addition to having rather more high frequency loss than CCDs, have considerably larger dark current variations from element to element when not illuminated.[2] While a dark current spike of 0.42% would probably be visible, it must be said that the largest such spike that has been observed in the sensors used in these experiments has been only 0.02%. Nevertheless, the dark current is strongly dependent on temperature, so it is not advisable to place the CCD where it will be subjected to a high ambient temperature. In extreme cases, cooling of the sensor with a small Peltier cooler could be considered.

3.6. Sensitivity variations

Because of mask tolerance in the manufacturing process and variations in the substrate, the sensitivities of the individual photosensitive elements are not all the same. The effect of these variations is to modulate the picture information

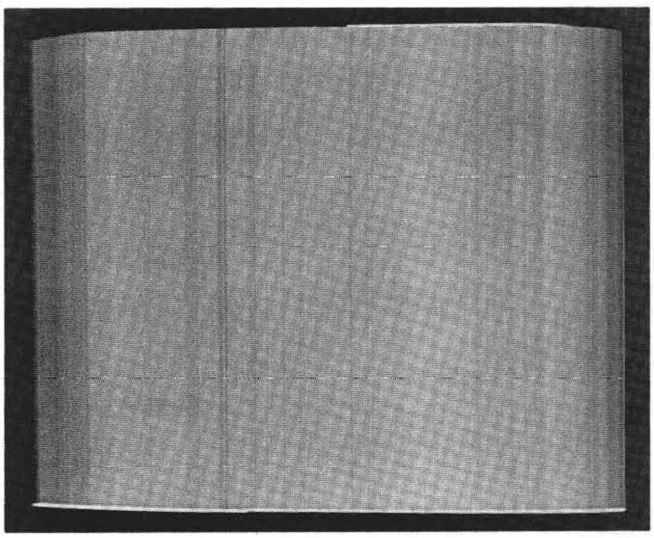

Fig. 11 - Sensitivity variations of CCD before correction

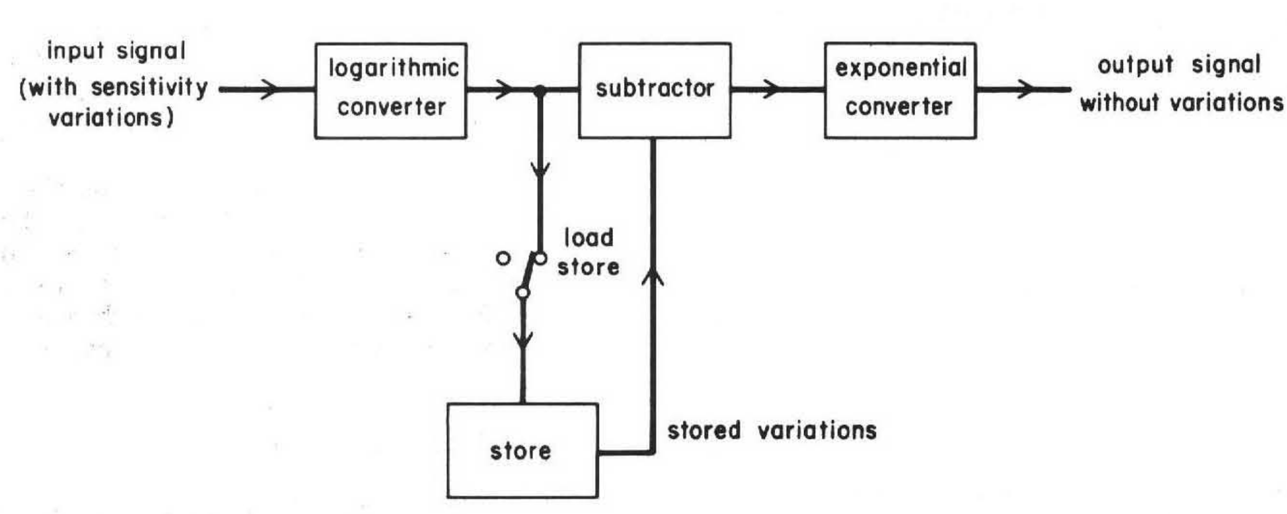

Fig. 12 - Block diagram of system used to remove sensitivity variations

with a fixed pattern which will appear as vertical stripes, visible mainly in the lighter areas of the final picture (see Fig. 11). These stripes can be removed[2] by storing the pattern in an 8-bit digital store and re-modulating the picture with the inverse of the stored sensitivity variations. The implications of this are more fully discussed in Appendix II.

A block diagram of a suitable system is shown in Fig. 12. The film is removed from the gate and the logarithm of the open gate signal written into the store. Subsequently this stored signal is subtracted from the log-converted output of the sensor in order to accomplish the correction. The result of using such a system is shown in Fig. 13. It should be noted at this point that correction in this manner will also remove any shading or vignetting due to non-uniform illumination. When used with a colour telecine it will also ensure a shading-free colour response over the whole picture.

3.7. Flare

Possible sources of flare are the sensor itself, the film and the copying lens, together with any mirrors that are present in the optical path. The sensor chip has negligible flare; the response of an element to light falling on adjacent elements is almost non-existent. Flare due to the film is a defect of the film and not the telecine; it will be reproduced in any design of telecine. Thus the only significant flare is produced by the copying lens and the window of the sensor; this leads to very low levels of overall flare. Fig. 14(*a*) shows the edge of a black to white transition made from a metal mask. The total clear area was approximately 50% of the film frame area. Fig. 14(*b*) shows the same edge but magnified in both directions. It may be seen that the flare falls to less than 1% of the peak illumination level at any position more than 0.5% of picture width from the edge of the transition.

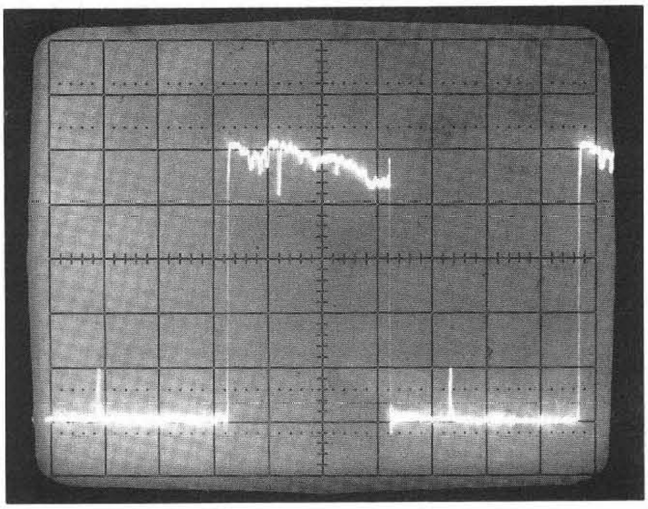

(*a*)

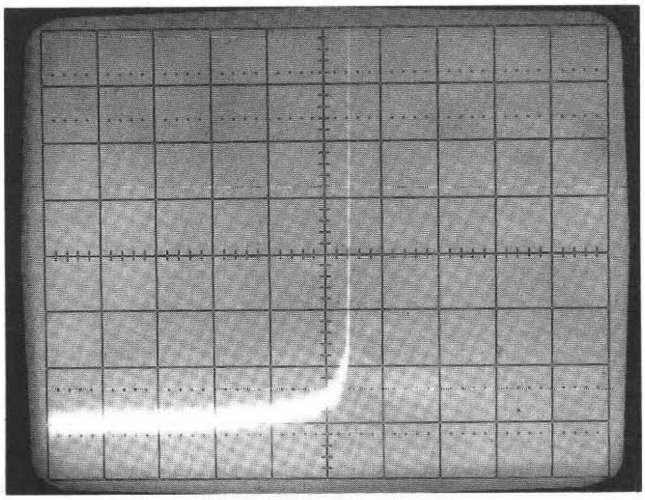

(*b*)

Fig. 14 - Flare performance of experimental scanner

(a) Output of scanner with metal mask in gate
Scales = horizontal 10 μs/div., vertical 0.2 V/div.

(b) Expanded view of edge of characteristic shown in (a)
Scales = horizontal 1 μs/div., vertical 10 mV/div.

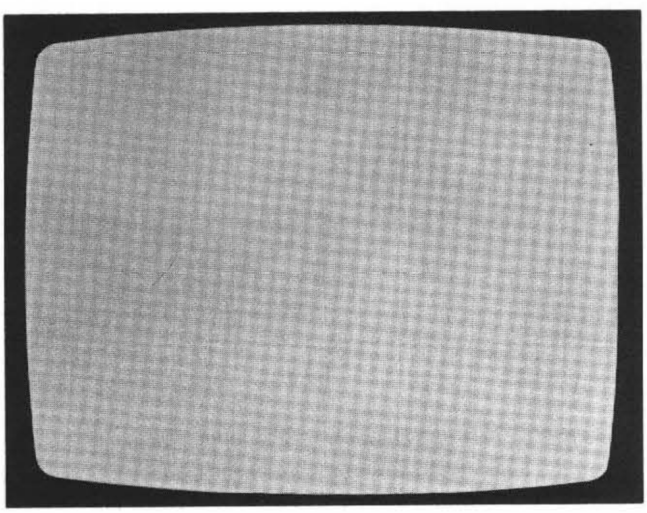

Fig. 13 - Sensitivity variations after correction

4. Colour operation

The performance of the monochrome telecine was sufficiently encouraging to justify the purchase of two further sensors in order to extend the

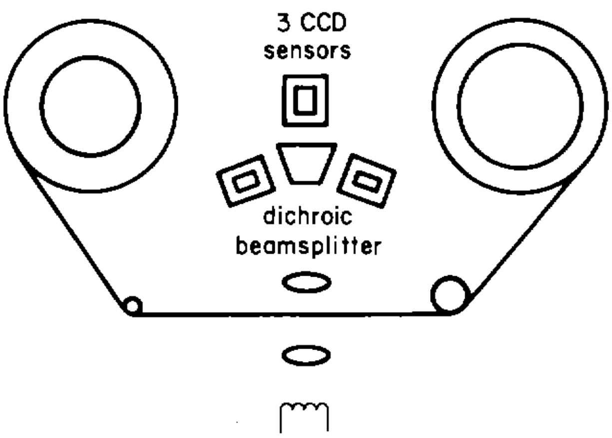

Fig. 15 - Modification for colour operation

experiments to colour operation. The single sensor of Fig. 1 was replaced by the arrangement of Fig. 15. Three sensors are required, one for each of the primary colours; a colour splitting block separates these red, green and blue components from the incident light. The signals from each of the sensors are then corrected for the variations in sensitivity from element to element and, still on the sequential standard, are processed in the normal way. Finally they are converted to a standard 625-line interlaced form.

Colour operation in this manner was first demonstrated at the International Broadcasting Convention 1978 in London. The scanning standard used was 625-lines 50 fields/sec and 16 mm film was shown at a speed of 25 frames/sec using digital storage to convert the signals to interlaced form. Aspects of colour operation will now be considered with particular reference to registration, colour analysis, signal-to-noise ratio and the particular requirements for improved sensors in the future.

4.1. Registration

Present day television cameras can attain very high registration performance; errors of less than 0.04% of picture width are commonly obtained in the central areas of the image, falling off to 0.15% at the extreme edges of the picture area. If at least the same performance is to be obtained from a CCD telecine then considerable mechanical precision is required in the mounting of the sensors. It is therefore natural to ask whether it is possible to register the sensors electrically.

It would be possible to carry out horizontal registration adjustments by altering the drive signals to the three CCD's independently. Correction of vertical registration errors would, however, involve introducing differential time delays into the three signals; these could be corrected in the sequential-to-interlace converter. Correction for rotational errors cannot be carried out in this way, however, and the electrical processing would be made much more complemented than it need be. Also, because the three colour signals would not be correctly timed before sequential-to-interlace conversion, operations involving addition of these signals (such as colour correction) could only be carried out after sequential-to-interlace conversion; the sequential-to-interlace converter itself would require a greater amount of storage, as the simplification of Y U V processing (which will be described later) could not be used. For all these reasons, mechanical adjustment of registration is preferable to electrical adjustment.

In order to register the images at the centre of the screen only two adjustments are needed; these

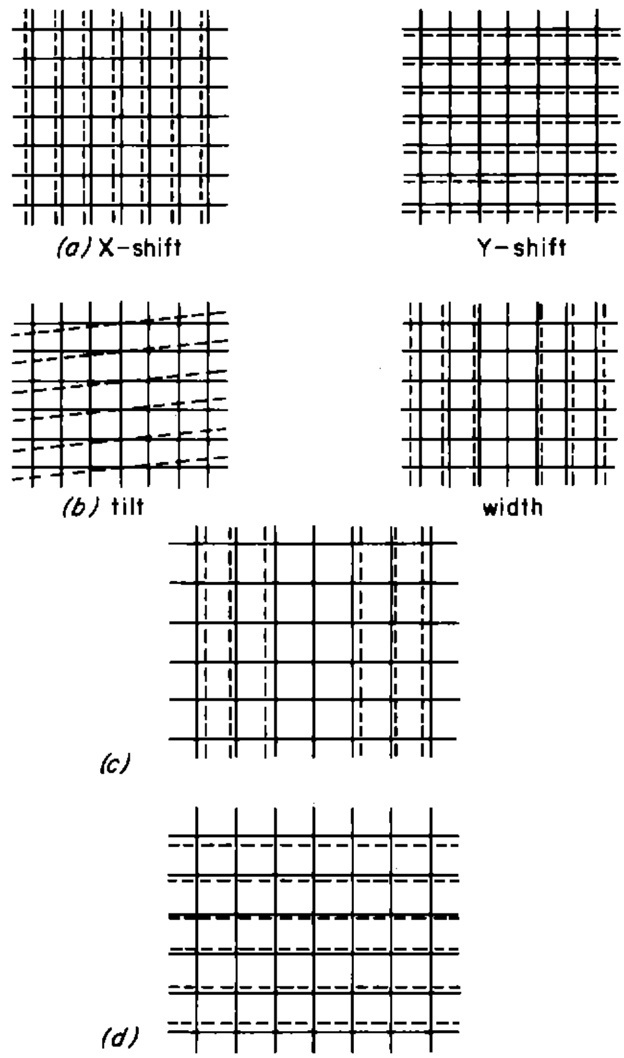

Fig. 16 - Types of registration error

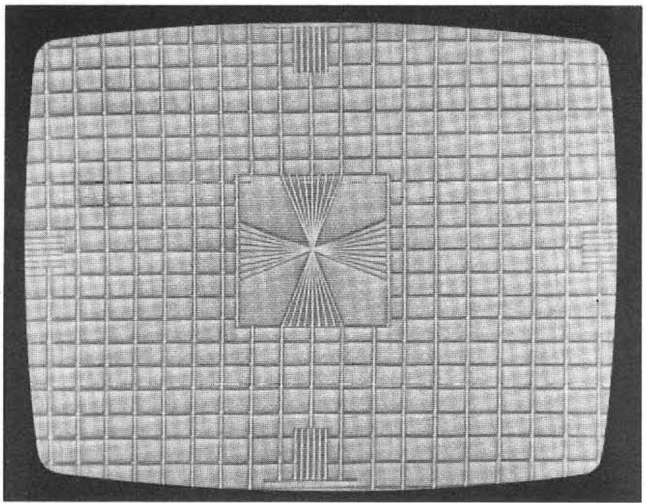

(a)

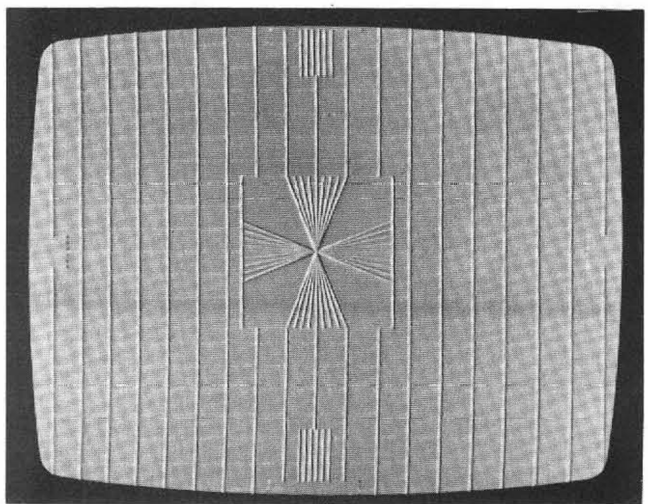

(b)

Fig. 17 - Registration performance of experimental telecine

(a) Difference between red and green output . (b) Green output subtracted from a delayed (20 ns) version of itself

are an X-shift and a Y-shift and are shown diagrammatically in Fig. 16(*a*). The accuracy of positioning needs to be approximately $\pm 5\mu m$ (or about ± 0.2 thousandths of an inch) for errors of less than 0.04% of picture width to be achieved.

Registration of the left and right-hand edges of the screen requires two other controls. These are a tilt and a width control, shown in Fig. 16(*b*). The tilt control implies a rotation of the sensor and is easily achieved. The width control is only achievable by moving the sensor towards or away from the copying lens and this will also affect the image focus. However variations in width between the three channels can only be caused by optical aberrations as CCD's are made to very precise dimensions. In the experimental telecine these optical aberrations were not present

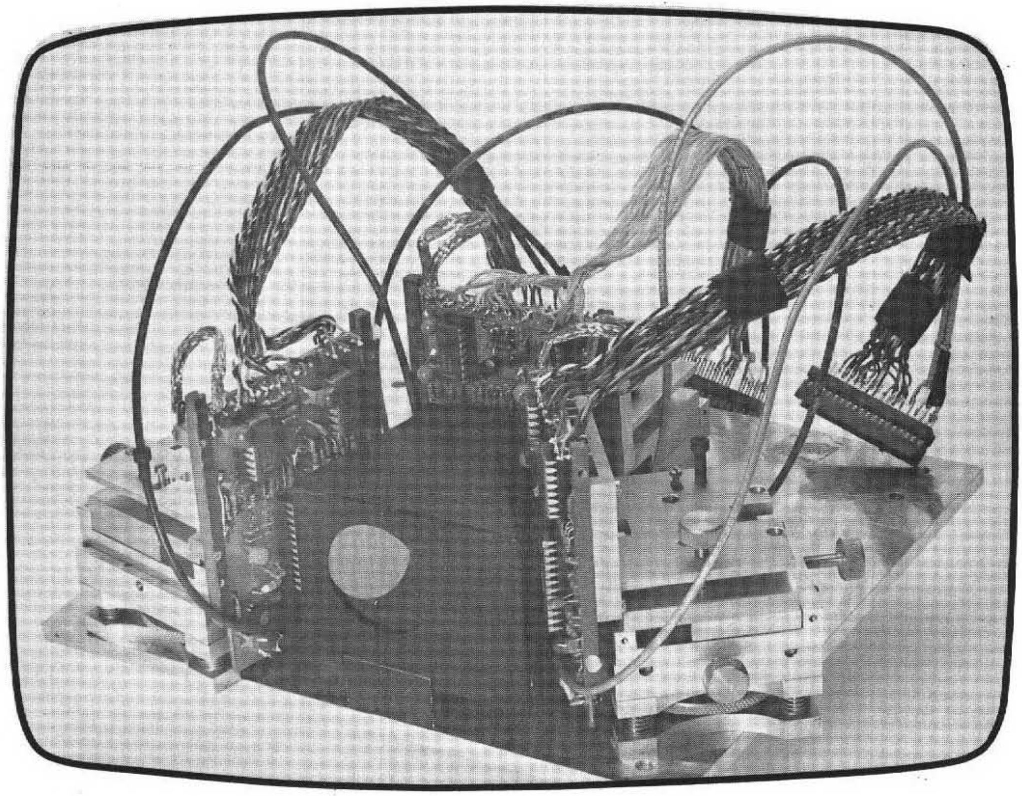

Fig. 18 - Colour splitting and sensor assembly

to any significant extent; when the three images were in focus the widths were all correct.

Likewise any second-order errors (illustrated for example in Fig. 16(*c*)) can only be caused by optical aberrations; again no significant errors were found. Finally any errors of the form shown in Fig. 16(*d*) where the registration varies up and down the picture are impossible, because the vertical scan is carried out by physical movement of the film.

Fig. 17(*a*) shows a photograph of the difference between the outputs of the red and green sensors. Comparison with Fig. 17(*b*), which corresponds to a constant horizontal mis-registration of 20 ns, indicates that the telecine errors are well within this figure. The registration was stable from day to day without any long term drift. The only errors noticed were short-term drifts due to differential thermal expansion while the mounting system was not in thermal equilibrium; it is felt that these should be able to be eliminated in future designs, if necessary by incorporating temperature control of the sensor assembly. Fig. 18 shows the complete assembly, which consists of the three sensors with their associated drive circuitry mounted around a colour splitter block.

The splitter block is one of the key components of the telecine; its characteristics help to determine the overall colour analysis and the factors which determine the design of the colour splitting system will now be discussed.

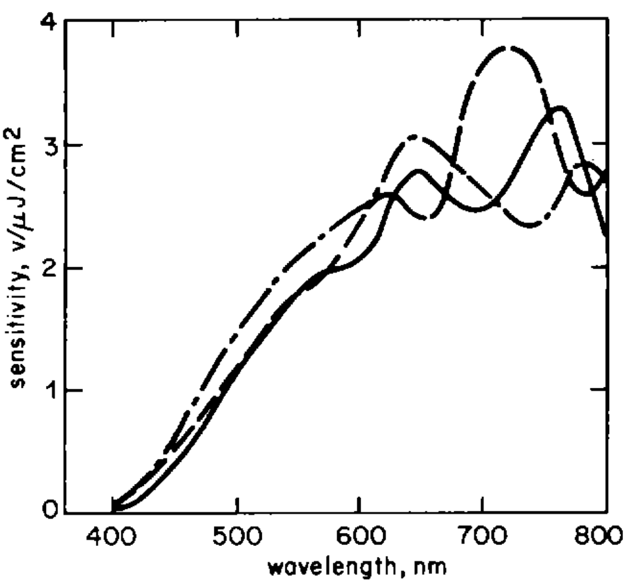

Fig. 19 - Spectral sensitivity of three CCDs
(——— CCD1 — — CCD2 —·— CCD3)

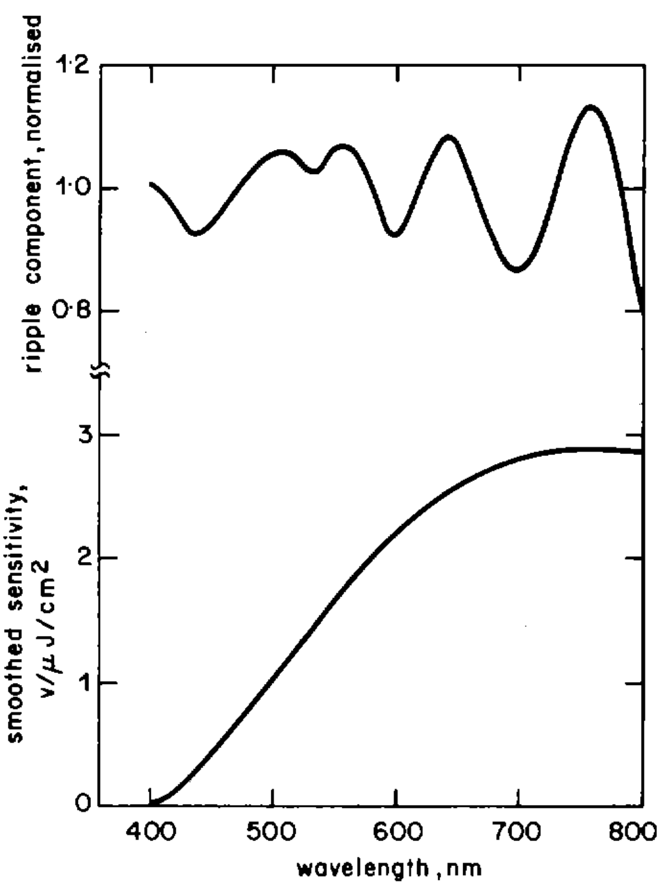

Fig. 20 - Components of spectral sensitivity for CCD1

4.2. Colour analysis

Fig. 19 shows the spectral sensitivity curves of the three sensors used in the telecine. The ripples in the curves are typical of CCD's using polysilicon electrode structures, as is the very low blue sensitivity. Both of these features create problems in designing a colour analysis system.

Fig. 20 shows one of the curves of Fig. 19 split into two components; these are an overall sensitivity curve common to all sensors (caused by the response of a silicon detector and the transmission of the polysilicon coating) and a ripple component which is unique to each sensor caused by multiple reflection in the electrode structure. The overall sensitivity curve may be incorporated in the design of the colour analysis; the ripple components should not be incorporated, as they will vary from sensor to sensor. Nevertheless the ripples will affect the colour analysis. For this reason the sensors need to be selected for each channel so that the ripple component has minimum effect; this is so when the region of interest lies either on a peak or in a trough of the ripple. Clearly a peak is the more desirable

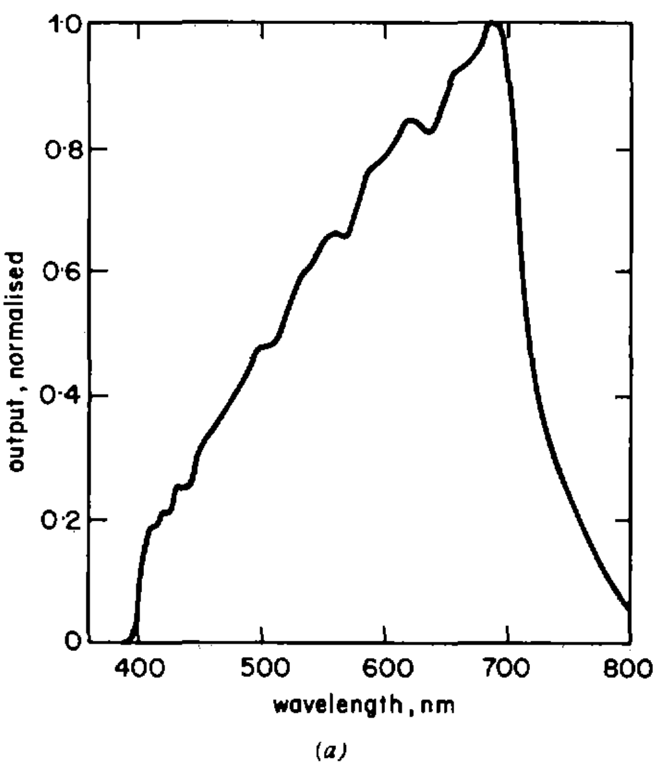

Fig. 21

(a) Light source output (b) Optical system transmission

of the two cases as the sensitivity will be higher. Thus CCD3 of Fig. 19 is most suitable for the blue channel as it has the highest sensitivity around 450 nm; CCD1 has a peak around 550 nm and is therefore used in the green channel. CCD2 with a peak at 620 nm is used in the red channel. If the sensors are selected in this fashion the variation in colour analysis from machine to machine should be no more than that caused by variations between individual colour splitter blocks.

The low blue sensitivity causes more of a problem, however. The situation is not helped by the fact that the light source used (a quartz-halogen projector lamp) has its lowest output in the blue region of the spectrum. Likewise most lenses will have the highest transmission in the green region of the spectrum and the transmission will fall off for shorter wavelengths. Fig. 21(*a*) shows the emission characteristics of the light source (together with a heat filter) and Fig. 21(*b*) shows the transmission of the optical system; it will be seen that, in both cases, the curves fall off towards the shorter wavelength end of the spectrum. The combined effect of these deficiences tends to push the main lobe of the blue analysis towards the green region of the spectrum.

It was clearly desirable to use a standard colour splitting block if possible since special-purpose blocks are expensive to manufacture. The characteristics of the block used are shown in Fig. 22. The blue analysis shows a significant subsidiary lobe below 700 nm due to light leakage in the block; in addition it is desirable to limit the red response in this region to avoid problems with the transmission of the film dyes to far-red light. The best solution was to filter the light source so as to exclude all wavelengths longer than about 650 nm. The nearest readily available filter had a slightly lower cut-off of 620 nm. This gave the overall analysis shown in Fig. 23.

This analysis was found to give reasonable results but the blue peak is rather closer to green than is usual; the main effect of this is to produce slightly desaturated pictures. If colour correction by matrixing the linear red, green and blue signals is carried out, an acceptable 'as optical' telecine is produced. Figs. 24(*a*) and 24(*b*) show the colour errors of several test colours before and after such colour correction. Alternatively it is possible to carry out colour masking by matrixing the logarithms of the three signals;[12] this will also correct for deficiencies in the film dye characteristics. This approach was verified experimentally and also found to give good results.

If optical shaping filters are included after the splitter block, it is possible to improve the

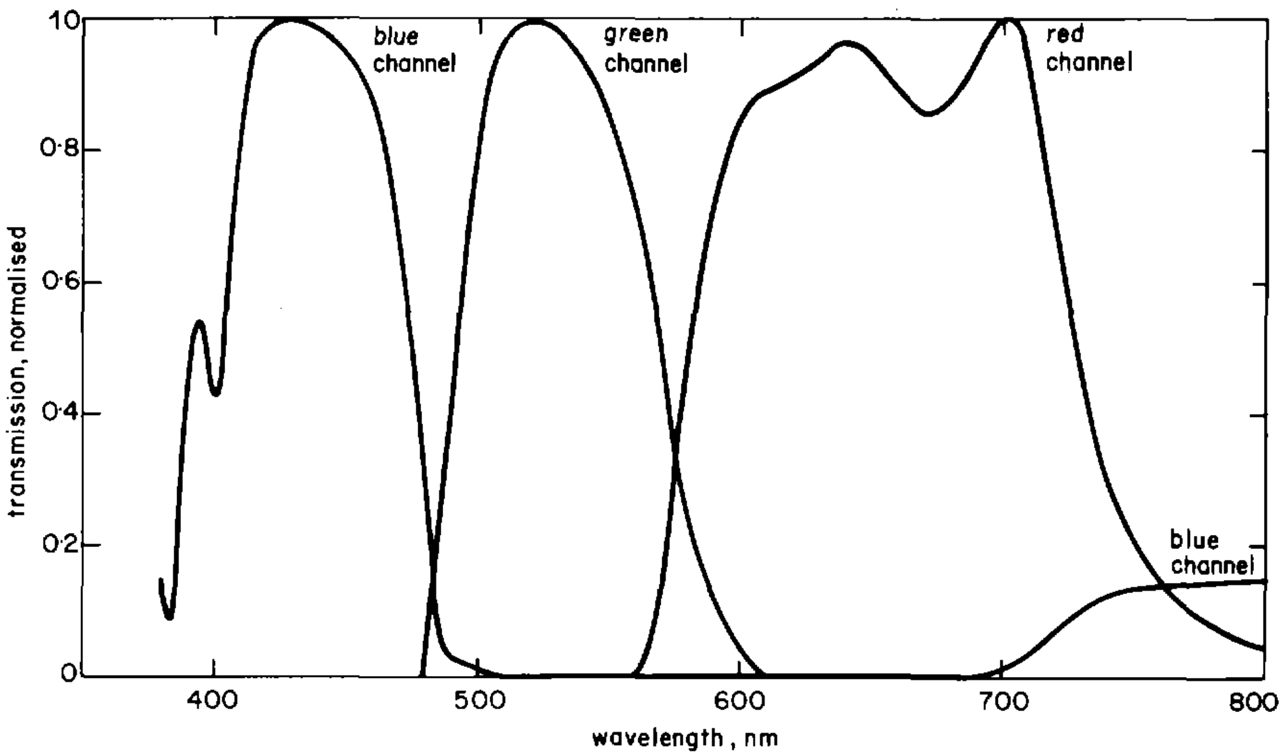

Fig. 22 - Spectral characteristics of splitter block

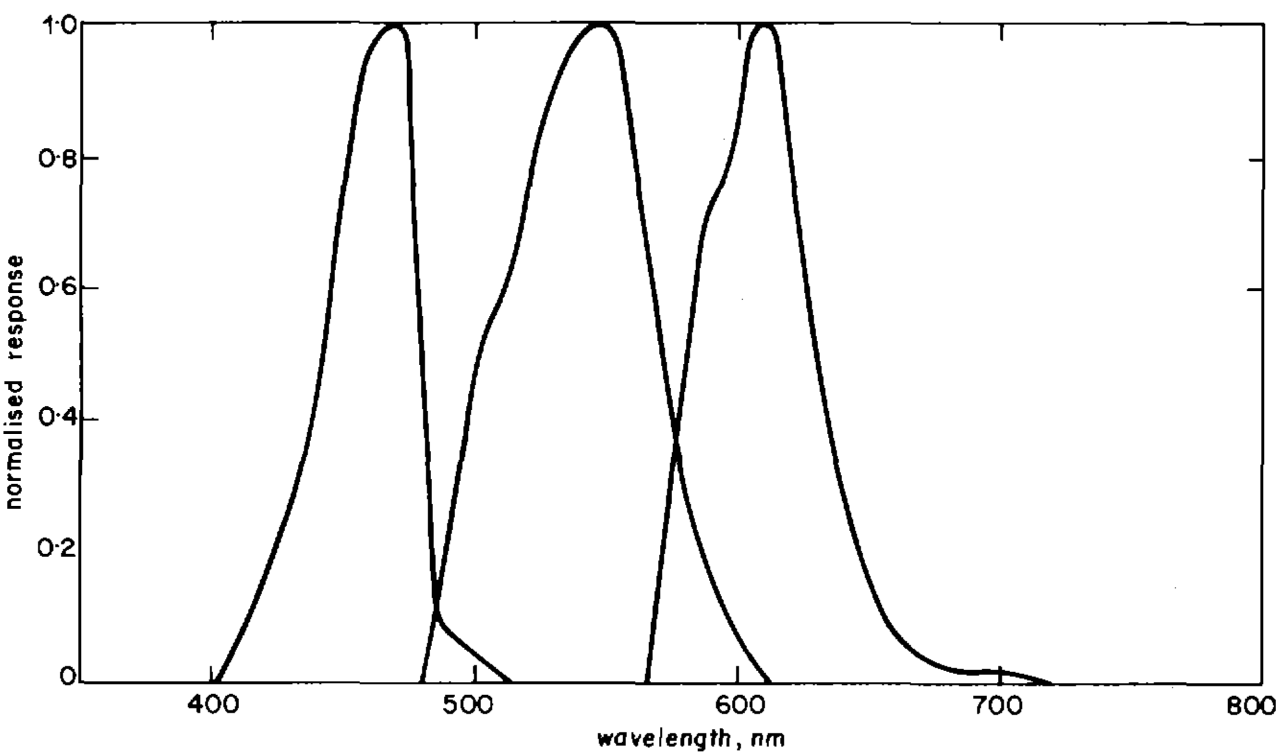

Fig. 23 - Overall colour analysis of telecine

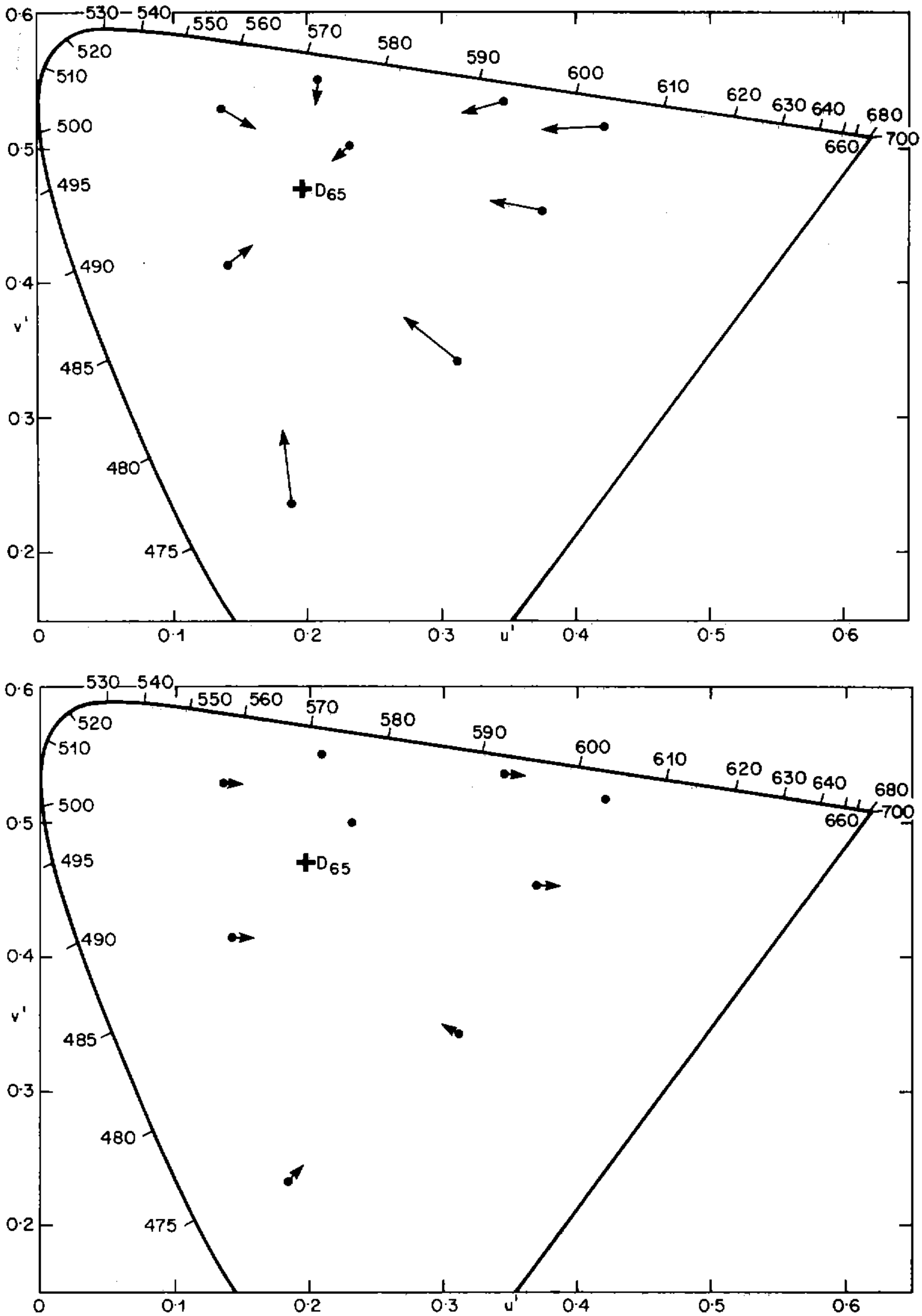

(a)

(b)

Fig. 24 - Colour changes produced by analysis of Fig. 23

(a) Before colour correction
(b) After colour correction

• original colour
→ reproduced colour

red analysis slightly, although if the peak is moved out further than about 630 nm the colour performance is made considerably worse. It is doubtful whether the blue analysis can be improved, however, as incorporating a shaping filter in the blue channel will cut down the light available considerably, thus increasing the noise unacceptably. The only hope of improving the blue analysis lies in the possibility of obtaining sensors with improved blue response. Nevertheless, it is encouraging how good the performance is, considering that the system uses 'off-the-shelf' components.

4.3. Noise performance

There are two main sources of noise in CCD sensors. The first is the noise arising from the discrete nature of the incident illumination (photon noise). The characteristics of this type of noise are that it increases as the square-root of the light level and that it has a flat frequency spectrum. From data supplied by the manufacturer the signal to noise ratio of the CCD when illuminated to near saturation level would be approximately 58 dB. In practice this photon noise is of little significance compared to the second noise source which is the electrical noise generated in the CCD.

This electrical noise has, in common with many other solid-state devices, a frequency spectrum which increases at low frequencies. Fig. 25 shows the spectrum of the noise from one sensor and it will be seen that components below 100 kHz are greater by up to 20 dB than components at higher frequencies. In addition the noise is independent of signal level at the output. The effect of gamma correction is then to modify the noise amplitude depending on the signal level; signals near white level will have the added noise amplitude reduced by up to 8 dB (assuming correction to a gamma of 0.4), signals from film of unit density will have the noise increased by about 4 dB and signals near black will have the noise increased by an arbitrary amount depending on the maximum gain available from the gamma corrector which is, in turn, dependent on the designed dynamic range.

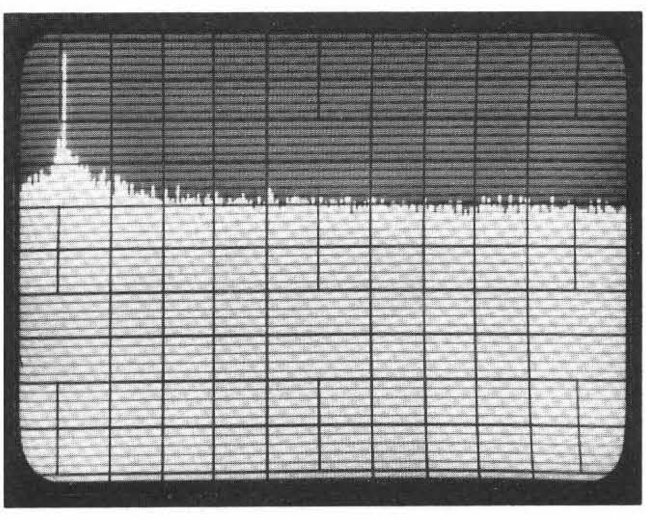

Fig. 25 - Noise spectrum from a CCD sensor
Vertical scale 10 dB/major div.
Horizontal scale 50 kHz/div. – Peak is at zero frequency

The overall effect is to introduce an obtrusive amount of low-frequency noise in areas of low luminance. This noise will be subjectively more annoying than its level might suggest, because of its low-frequency nature (preliminary tests indicate that the impairment due to this unusual noise spectrum may be equivalent to white noise as much as 20 dB higher in level). Because of this, measured figures can be misleading. For example, the measured value of the unweighted r.m.s. noise in a 5.5 MHz bandwidth was 72 dB below the maximum signal level at the output of the red and green sensors (because of the reduced sensitivity to blue light, the blue channel could not be driven to more than 20% of saturation level and so the noise level was only 58 dB below maximum signal level). At first sight, these figures would indicate an exceptionally good signal-to-noise performance. Nevertheless comparison with a flying spot telecine (whose signal-to-noise ratio is typically 48 dB when reproducing film of unity density) indicates that the visibility of the noise is rather less than for a CCD telecine.

Aperture correction will, of course, further worsen the signal-to-noise ratio; horizontal aperture correction will not be so bad as vertical aperture correction since horizontal correction will mainly boost the high frequency noise which is not present to such a large extent.

Another unpleasant feature of the noise is that it is concentrated in the blue channel. As well as slightly increasing the total subjective perception of noise itself, this tends to make dark areas of the picture look more blue than they should be, due to rectification of the noise by the display non-linearity.

It seems likely that, in the near future, sensors with improved blue response will be available (see following Section). This will remove the unbalance in noise between the three channels or, at the very least, substantially reduce it but the effect on the overall lumi-

nance signal-to-noise ratio will not be large. A more effective approach would be to increase the sensitivity of the on-chip output amplifier, or to decrease its noise level. It is likely that this will be accomplished in forthcoming CCD's; preliminary data on one such device indicates an improvement in signal-to-noise ratio of 10 dB in addition to that obtained by the improved blue response.

4.4. Effect of improved sensors

Sensors are now starting to become available which have improved response to blue light. The usual way in which this is done[13] is by using photodiodes as the light sensing elements but retaining the CCD output structure. By this means the polysilicon electrodes covering the photosensitive region are eliminated; thus the quantum efficiency to blue light is raised and the ripples in the spectral characteristic considerably reduced.

Because the ripples are reduced, selection of devices will no longer be needed. The improved blue response will lead to less noise in the blue channel and some increase in the green signal output will also be obtained.

In order to estimate what the performance of a telecine using such sensors could be, sensors with a response as shown in Fig. 26 were assumed (this being typical of sensors currently offered). The same optical system and splitter block were also assumed, but the lenses were assumed to be coated so as to optimise transmission at the blue end of the spectrum. A computer was then used to simulate the effect of these changes on the optical analysis.

Results were encouraging; green sensitivity was increased slightly and blue sensitivity by a factor of three (thus increasing the blue signal-to-noise ratio to 68 dB). The coefficients of the colour-correction matrix were slightly reduced (which will lead to a further slight reduction in noise level) although the colour performance was slightly inferior to the previous case.

The overall optical analysis of the system is shown in Fig. 27; some adjustment of the analysis characteristics by including shaping filters would improve the colour performance, at the expense of reducing the signal level.

4.5. Sequential to interlace conversion

The basic concept of sequential to interlace conversion is the same for colour operation as for monochrome operation; the only difference is that there are now three signals to be converted. In order to avoid the need for three time the previous amount of storage, however, the red, green and blue signals can be matrixed to form a luminance and two colour-difference signals. The colour difference signals can then be filtered to

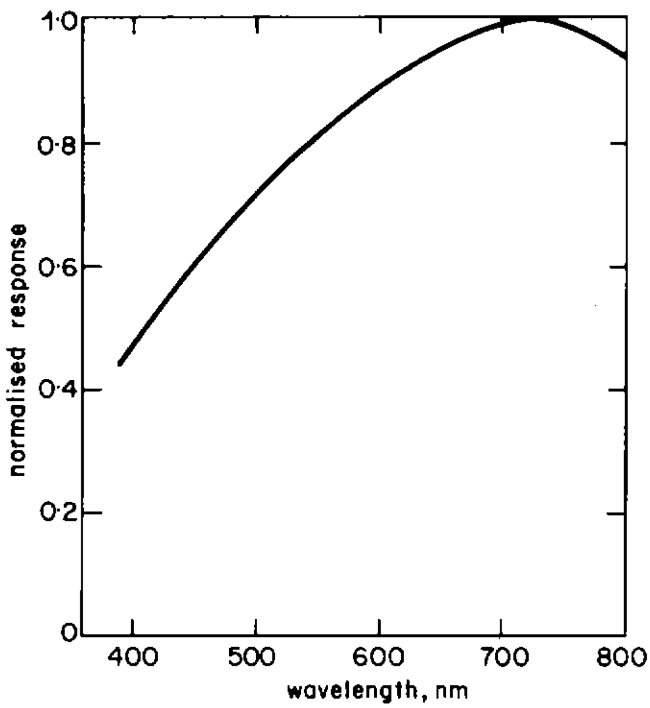

Fig. 26 - Spectral response assumed for improved sensors

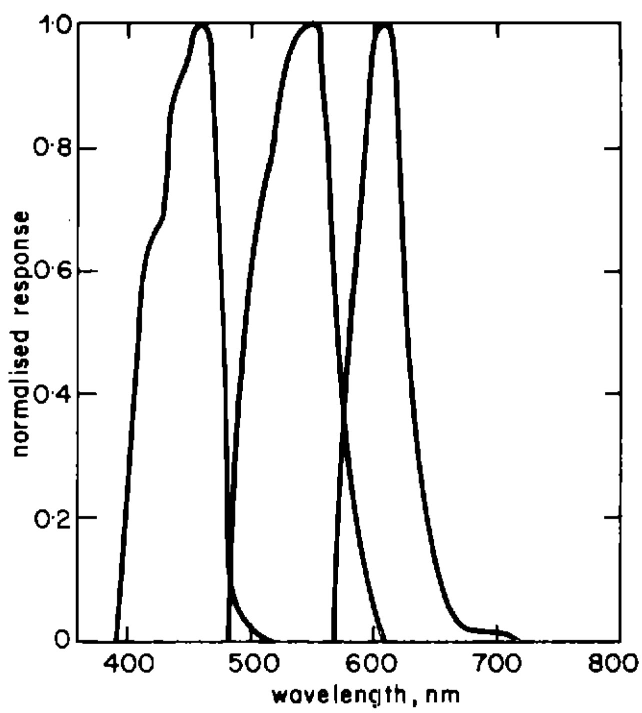

Fig. 27 - Optical analysis using sensors of Fig. 26

a lower bandwidth; by this means both signals can be fitted into the same amount of storage as the luminance signal. The storage requirement is then only twice that for monochrome signals.

5. Conclusions

Solid-state sensors can be used to produce full resolution broadcast-quality pictures from film. Some of the signal processing required is at present rather expensive. A digital field-store, for example, has been used to obtain 50 fields/sec interlaced pictures from sequential scanning of the film at 25 frames/sec. However, the machine is optically and mechanically simple and this feature may well justify the additional cost of the signal processing. Alternatively, at the expense of increased mechanical and optical complexity in the form of an oscillating mirror or rotating optical polygon, interlaced scanning could be achieved directly. In this event, however, it is certain that the picture quality would be degraded by additional flare, unsteadiness, and flicker.

In spite of the poor blue response of present day CCDs it has been found possible to achieve good colour reproduction using a standard colour splitting prism and infra-red filter, together with a small degree of colour correction. Sensors having improved blue sensitivity will ease the situation.

The principal disadvantage of this approach is that the noise level is slightly higher than in a flying-spot telecine. While the introduction of sensors with improved blue sensitivity will help to equalise the noise levels in the red, green and blue channels, the overall visibility of noise will be little affected. In order to overcome this, sensors with lower levels of electrical noise are required; it seems likely that such sensors will soon become available.

A further disadvantage is that registration of three sensors is required. This is a simpler operation than for a camera, however, and has proved relatively easy to achieve in practice.

Advantages are numerous. There would be virtually no maintenance with no gradual deterioration of performance due to tube ageing. There would be completely uniform focus over the entire field apart from optical aberrations. Electronic compensation for element to element sensitivity variations would also result in a uniform signal output over the entire field, with no shading or vignetting due to non-uniform illumination. There would also be no geometric or optical transmission mismatch between odd and even fields as can occur with a flying-spot telecine. The running cost should be very low, since the only replacement requirement will be the light source.

6. References

1. WRIGHT, D.T. 1973. Solid-state sensors: the use of a single dimension 512 element array for film scanning. BBC Research Department Report No. 1973/32.

2. LE COUTEUR, G.M. 1976. Solid state image sensors : improvements in signal processing techniques. BBC Research Department Report No. 1976/4.

3. LE COUTEUR, G.M. 1976. Performance tests on a selection of 100-element charge-coupled devices. BBC Research Department Report No. 1976/23.

4. CHILDS, I. *and* SANDERS, J.R. 1978. An experimental telecine using a line-array CCD sensor. *SMPTE Journal*, 1978, **87**, 4, pp. 209 – 213.

5. SEQUIN, C.H. *and* TOMPSETT, M.F. 1975. Charge transfer devices. Supplement 8 to advances in Electronics and Electron Physics, New York, Academic Press, 1975.

6. KOSONOCKY, W.F. *and* CARNES, J.E. 1972. Two-phase charge-coupled shift registers. 1972. IEEE International Solid State Circuits Conference Digest, p. 132, IEEE, New York.

7. KRAMBECK, R.H., WALDEN, R.H. *and* PICKAR, K.A. 1971. Implanted barrier two-phase charge-coupled device. *Applied Phys. Letts.*, 1971, **19**, 12, pp. 520 – 522.

8. WALDEN, R.H. et al. 1972. The buried-channel charge-coupled device. *Bell Syst. Tech. J.*, 1972, **51**, 7, pp. 1635 – 1640.

9. ESSER, L.J.M. 1973. The peristaltic charge-coupled device. Proceedings of the Charge-Coupled Device Applications Conference, San Diego, 1973, pp. 269 – 277.

10. LE COUTEUR, G.M. 1978. Sampling frequencies and structures for solid state image sensing in broadcasting. BBC Research Department Report No. 1978/2.

11. OLIPHANT, A. 1978. A digital telecine processing channel. BBC Research Department Report No. 1978/9.

12. MARSDEN, R.P. 1975. Electronic masking for telecine : a review of masking for positive and negative film. BBC Research Department Report No. 1975/16.

13. SUZUKI, N. 1977. New 1024-element charge coupled linear image sensor with high sensitivity. *Electronics Letters*, 1977, **13**, 24, pp. 716 – 17.

Appendix I

Calculation of Optimum Vertical Aperture

The vertical spatial frequency response of the sensor/film transport combination is obtained by taking the Fourier transform of the spatial aperture shown in Fig. 9. For all the cases shown in this figure (referring to different sizes of sensor element as compared to a television line width) the overall shape of the Fourier transform is given by

$$F(f) = \frac{\sin(\pi w_t f)}{\pi w_t f} \cdot \frac{\sin(\pi w_s f)}{\pi w_s f} \qquad (1)$$

Where $F(f)$ is the response at a spatial frequency of f (cycles/mm) and w_t and w_s are the widths of a television line and a sensor element respectively (in mm). This equation does not take into account the overall magnitude of the response which will increase as the sensor width increases and more light is collected. Thus we need to define the vertical spatial frequency response by a new function, $F'(f)$, given by

$$F'(f) = K_s \cdot w_s \cdot F(f) \qquad (2)$$

If the output of the sensor is passed through an aperture corrector which exactly compensates for the loss in response of the sensor/film transport at high vertical frequencies, the aperture corrector will have a response, $G(f)$, given by

$$G(f) = \frac{1}{F(f)} \qquad (3)$$

The signal level is then constant for all vertical frequencies at a value proportional to w_s. The noise level is however dependent on the characteristics of $G(f)$. If we assume that it was initially white noise then, after aperture correction, the total noise level, N_T, becomes

$$N_T = K_N \sqrt{\int_0^{\frac{1}{2w_t}} G^2(f)\, df} \qquad (4)$$

(K_N is a constant)

Thus the signal-to-noise ratio, $r_{S/N}$, is given by

$$r_{S/N} \propto \frac{w_s}{N_T} \propto \frac{w_s}{\sqrt{\int_0^{\frac{1}{2w_t}} \left[\frac{\pi w_t f}{\sin \pi w_t f} \cdot \frac{\pi w_s f}{\sin \pi w_s f}\right]^2 df}} \qquad (5)$$

This function was calculated numerically for different ratios of w_s to w_t and the results are plotted in Fig. 28. It is seen that the signal-to-noise ratio is optimum when the sensor element width is slightly greater than that of a television film line but that this optimum is fairly broad.

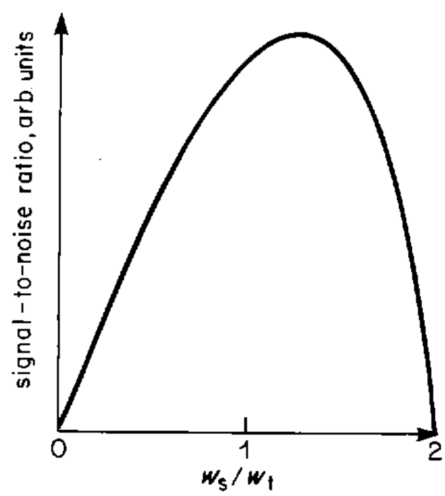

Fig. 28 - Signal-to-noise ratio as a function of sensor width

Appendix II

Correction of Sensitivity Variations

In an ideal sensor the output would consist of an electrical signal related to the optical intensity profile along the length of the sensor multiplied by a regular series of equal height impulses corresponding to the samples taken by the individual sensing elements. The frequency spectrum of the output will then consist of the original optical signal spectrum convolved with the spectrum of the impulses (see Fig. 29(*a*), (*b*) and (*c*)).

However, in a practical sensor the sensitivities of the elements are not all equal and hence the heights of the various impulses multiplying the optical intensity profile are no longer constant. This gives rise to the modified sampling spectrum shown in Fig. 29(*d*); when this modified spectrum is convolved with the input spectrum the result is as shown in Fig. 29(*e*). There is considerable distortion of the output signal.

The only exact way of correcting the output spectrum of Fig. 29(*c*) is to correct the sensitivities of each individual element, i.e. to multiply the samples as they emerge from the sensor by a set of stored values such that the combined effect is to convert all the sampling impulses to an equal height. This presents considerable practical difficulties, however, and so an alternative was considered.

In this alternative method, the signal of Fig. 29(*e*) is first lowpass filtered to give the signal shown in Fig. 29(*f*). This signal is then corrected for sensitivity variations to give the final signal shown in Fig. 29(*g*). The subsidiary lobes which appear are caused by the error introduced by truncating the original signal spectrum and are related to the optical input signal. If the optical input contained few high frequencies and if the correction is carried out for a bandwidth rather greater than that finally required (5.5 MHz) then these error components can be made to be outside the video bandwidth. In areas of high picture detail, however, the error components will stray into the video bandwidth re-introducing sensitivity variations (although in a modified form which will not necessarily appear as vertical stripes). It is doubtful whether these will be visible, bearing in mind the masking effect of the picture detail, and so this alternative approach would appear to be perfectly satisfactory.

This approach is, in fact, the one that has been used in the work described in this Report. The errors introduced by the restricted correction bandwidth have never been visible using the available sensors.

SMW/VY

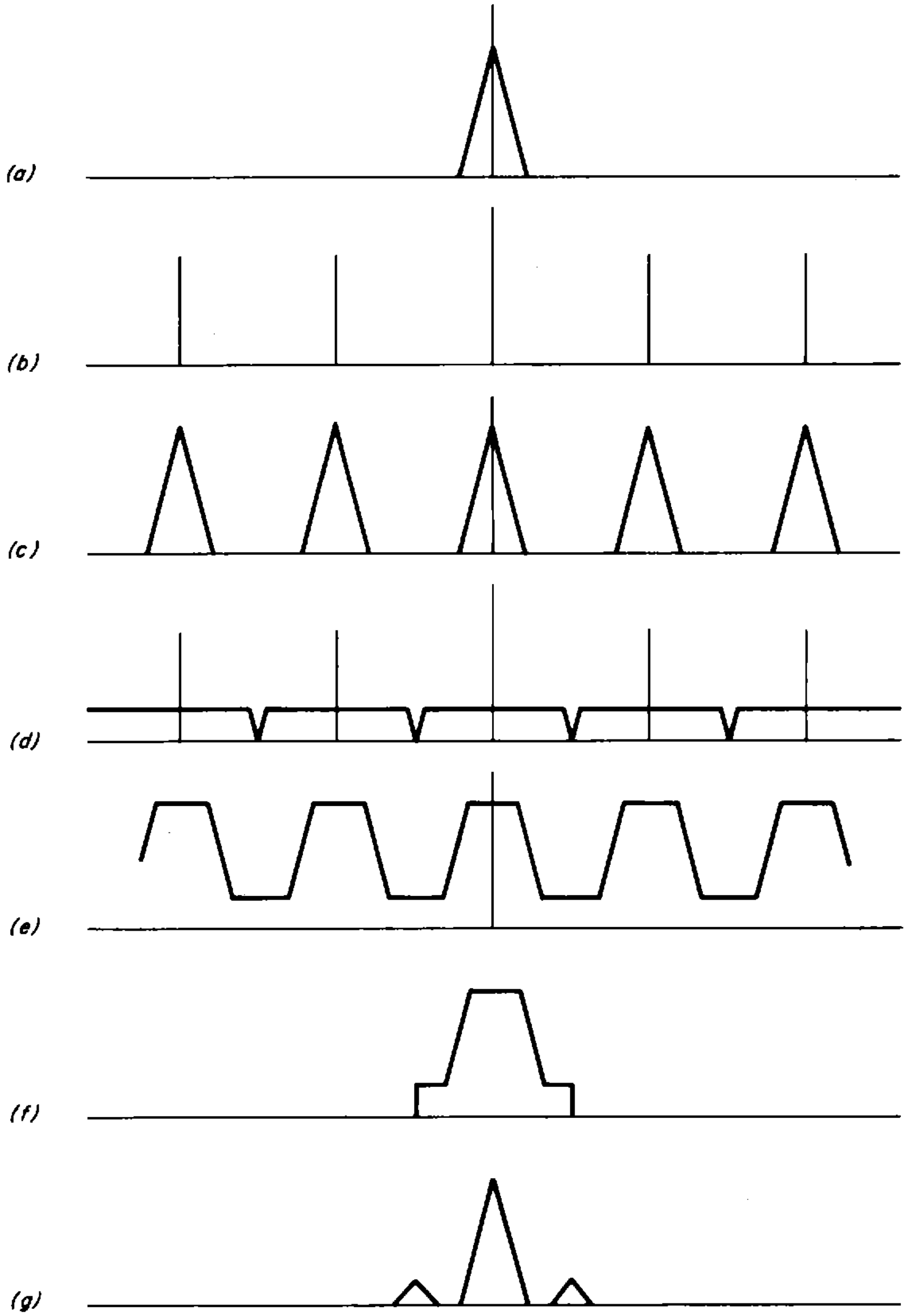

Fig. 29 - Frequency spectra of sensitivity correction signals

(a) optical input (b) sensor sampling spectrum (ideal sensor) (c) output of ideal sensor
(d) sensor sampling spectrum (with sensitivity variations) (e) output of sensor with sensitivity variations
(f) after lowpass filtering (g) corrected spectrum of lowpass filtered sensor

Printed by BBC RESEARCH DEPARTMENT, Kingswood Warren, Tadworth, Surrey, KT20 6NP